Macromolecules
ARTICLE

Macromolecules **2009**, *42*, 8181–8186 **8181**
DOI: 10.1021/ma901518w

Selective Synthesis of Poly(*m*-phenylene oxides) over Oxacalixarenes

Jay Wm. Wackerly, Joseph M. Meyer, W. Christian Crannell, Sarah B. King, and Jeffrey L. Katz*

Department of Chemistry, Colby College, 5754 Mayflower Hill Dr., Waterville, Maine 04901

Received July 13, 2009; Revised Manuscript Received August 28, 2009

ABSTRACT: We report a high yielding AA−BB type step-growth synthesis of poly(*m*-phenylene oxides) (*m*POs) by nucleophilic aromatic substitution (S_NAr) reactions. Previously, poly(*m*POs) have proven difficult to synthesize, especially by S_NAr, due to competing cyclooligomer (oxacalixarene) formation. We have found that the linear (polymeric) vs cyclic (oligomeric) product distribution is strongly dependent on the substitution pattern of the electrophilic monomer, and a model is described that predicts whether the reacting monomers will kinetically favor formation of poly(*m*POs) or oxacalixarenes. The polycondensation reaction tolerates a range of functional groups on both reactive monomers, and the synthesized poly(*m*POs) have high thermal and aqueous stability but are readily depolymerized in polar aprotic media.

Introduction

The synthesis and properties of poly(phenylene oxides) (PPOs) have been studied for over 50 years for their use as thermally stable polymeric materials.[1] Research in this area has mostly focused on *para*-linked systems, presumably due to their relative ease of synthesis. PPOs are currently synthesized industrially from 2,6-disubstituted phenols using copper as the oxidant,[2] but they have also been polymerized using other oxidants[1d] and under Ullman[1e] conditions. Notably, although nucleophilic aromatic substitution (S_NAr) reactions are extensively utilized for the industrial synthesis of many poly(aryl ethers) such as poly(aryl ether sulfones), poly(ether ether ketones), and poly(ether imides),[3] there are few reports of PPOs synthesized by S_NAr reactions.[4]

Far fewer examples of isomeric poly(*meta*-phenylene oxides) (*m*POs), which should be less prone to oxidation[5] than *para*-PPOs, have been reported. Reports from the 1960s discuss the synthesis of low molecular weight, unfunctionalized poly(*m*POs) by Ullman coupling.[6] A poly(*m*PO) containing a nitrile group on every other monomeric unit synthesized by S_NAr is commercially available from Idemitsu Kosan (PEN, poly(arylene ether nitrile),[7] and this same polymer was also synthesized by Kricheldorf and co-workers by S_NAr from a silylated 1,3-diphenol by fluoride-catalyzed polymerization.[8] Although the tensile strength and thermal stability are reported to make PEN suitable for use in engineering applications, no other poly(*m*POs) have since been made available commercially or have appeared in the literature.

Our group[9] and others[10] have shown that condensation of a 1:1 molar ratio of nucleophilic *m*-diphenol monomers (**1**) and electrophilic electron-deficient *m*-dihalide monomers (**2**) provides extremely high selectivity for oxacalix[4]arenes (**3**) under equilibrating (thermodynamic) conditions (Scheme 1). Under nonequilibrating (kinetic) conditions, mixtures of **3**, larger cyclic oligomers (oxacalix[6]arenes, oxacalix[8]arenes, etc.), and linear oligomers can be isolated.[9b,10g,i,j,m] The relative absence of reported poly(*m*POs) synthesized by S_NAr[11] appears to primarily reflect the propensity of these systems to form oxacalixarenes even when reacted at high concentrations. During attempts to selectively synthesize large oxacalix[*n*]arenes, we discovered an operationally simple, one-step AA−BB type step-growth polymerization that yields poly(*m*POs)[12] in high yields and containing diverse functionality. We herein describe the details of our synthetic investigations in forming poly(*m*POs). The synthesized polymers exhibit high thermal stabilities under a nitrogen atmosphere or in water but can be readily depolymerized in polar aprotic solvents. Further, the success or failure of S_NAr-based polycondensation reactions to yield poly(*m*POs) has been found to depend on the substitution pattern on the electrophilic *m*-dihalide monomer. We describe a model that predicts, based on the conformational preferences of the growing aryl ether chains, which systems can be driven to favor the formation of poly(*m*POs) over cyclic oligomers (oxacalixarenes).

Experimental Section

General Reaction Procedure for Poly(*m*PO) Formation. Under an inert atmosphere, 1.35 mmol of *m*-diphenol **5** (1 equiv), 1.35 mmol of the aryl *m*-dihalide **6** (1 equiv), and anhydrous DMSO (2.0 mL) were combined. Upon reaching solution homogeneity, 2 g of freshly, finely ground anhydrous K_2CO_3 (10 equiv) was added, and the flask was immediately placed in an oil bath at 100 °C. The reaction was stirred vigorously and quenched after 40 min by first adding additional DMSO (8 mL) and then precipitating the polymer into 100 mL of water. After thorough stirring to break up any large solid particles, the precipitate was collected by filtering the solution through a pad of Celite. The filter cake was then washed with acetone, dissolved in methylene chloride, filtered to remove the Celite, and concentrated in vacuo.

Results and Discussion

Poly(*m*PO) Synthesis. We have previously shown that condensation of *m*-diphenol orcinol (**5a**) with either 4,6-dichloropyrimidine (**6a**) or 2,6-dichloropyrazine (**7**) under thermodynamic S_NAr conditions produces the corresponding oxacalix[4]arenes in high yield, while kinetic conditions furnish mixtures of linear and cyclic oligomers.[9b] While investigating alternative kinetic reaction conditions,

---

*Corresponding author: Fax (207-859-5760); e-mail jlkatz@colby.edu.

Scheme 1. Oxacalix[4]arene Formation under Thermodynamic Control

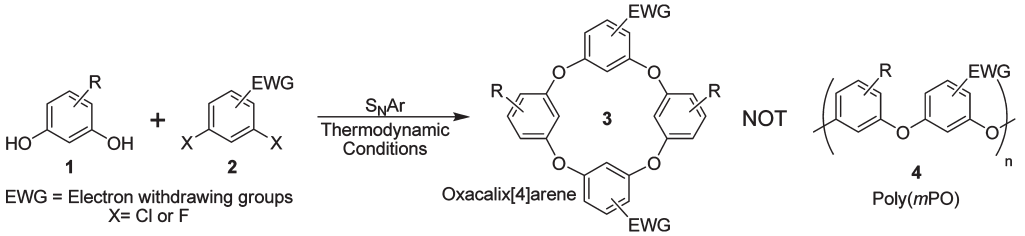

Scheme 2. High Yielding Syntheses of Polymeric *m*-Phenylene Oxide 8

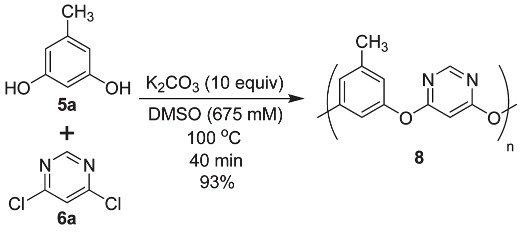

we noticed a divergence in reactivity between electrophiles 4,6-dichloropyrimidine (**6a**) and 2,6-dichloropyrazine (**7**). When employing electrophile **7**, increasing the reaction concentration and using excess base continued to furnish oligomeric mixtures (vide infra). However, conditions of high concentration and excess base using isomeric 4,6-dichloropyrimidine (**6a**) at short reaction times preferentially formed a different product than previously observed. NMR and GPC[13] analysis revealed that this product was poly(*m*PO) **8** (Scheme 2). Optimized polymerization conditions were found to require 10 equiv of base and a concentration of 675 mM, both with respect to the concentration of orcinol (**5a**). While the use of excess base is important for reaction efficiency, variation of the base identity (Cs_2CO_3, CsF, or K_2CO_3) did not have a significant deleterious effect on the yield of **8**. A concentration of 675 mM was considered optimal because this was the maximum concentration at which the reaction could be effectively stirred in order to obtain consistent results.[14] The temperature was also optimized to minimize the formation of the corresponding oxacalix[4]arene **9**[9b] (from **6a** + **5a**), which is formed preferentially at higher temperatures (i.e., above 100 °C) at short reaction times. DMF solvent could also be substituted for DMSO with a negligible effect on the yield of the polymer formed.[15]

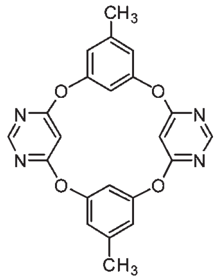

9

Kinetic studies were performed to ascertain the optimal time for polymerization. The reaction shown in Scheme 2 was conducted containing an internal standard and analyzed at different time points.[16] ^{1}H NMR (Figure 1[17]) and GPC (Figure S1) analysis show that at short reaction times a significant amount of dihalogenated linear trimer (A, Figure 1) and linear low molecular weight polymer (B, Figure 1) are formed with no evidence of any remaining monomer **6a**. As the reaction proceeds to the intermediate time points, one distinct ^{1}H resonance corresponding to poly(*m*PO) **8** predominates. At the later time points the polymer degrades, and increasing amounts of oxacalix[4]arene **9** are observed. Performing the reaction at 10-fold dilution for 20 h under the otherwise optimized conditions exclusively yields oxacalix[4]arene **9** (Figure S3), indicating that not only time but also concentration, and hence polymer solubility, is extremely important in governing the product obtained from the reaction. On the basis of the kinetic data, a 40 min reaction time was identified as optimal to achieve a high polymer to oxacalix[4]arene ratio while also minimizing the presence of linear oligomers.

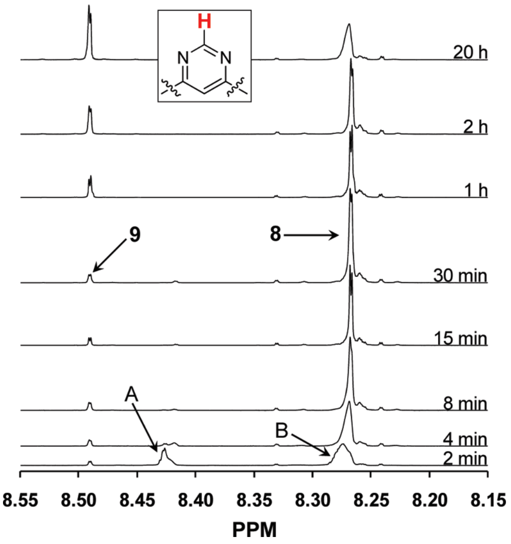

Figure 1. ^{1}H NMR spectra of the polymerization reaction from Scheme 2 analyzed at different reaction times. The spectral region shown corresponds to the shifts for the red proton. Oxacalix[4]arene (**9**), poly(*m*PO) (**8**), pyrimidine end groups of linear oligomers (A), and internal pyrimidine groups of linear oligomers (B) are labeled.

Poly(*m*PO) **8** can be easily separated from oligomeric contaminants and oxacalix[4]arene **9** by precipitation in water and washing the solid residue with acetone before isolating the white, filmy polymer in 93% yield and purity $> 95\%$. Analysis of the acetone wash reveals predominantly oxacalix[4]arene **9**. The synthesis of poly(*m*PO) **8** was also conducted on a 13.5 mmol scale (10-fold increase) and purified by column chromatography with only a minor loss of the polymer on the silica.[16]

The substituents on both the *m*-diphenol and 4,6-dichloropyrimidine monomers were varied to explore the scope of this poly(*m*PO) synthesis (Table 1). The 5-position functional group on the *m*-diphenol can be changed to an alternative hydrocarbon (R_1 = *n*-pentyl, **10**, 87%), electron withdrawing (R_1 = CO_2Me, **11**, 92%), or electron donating

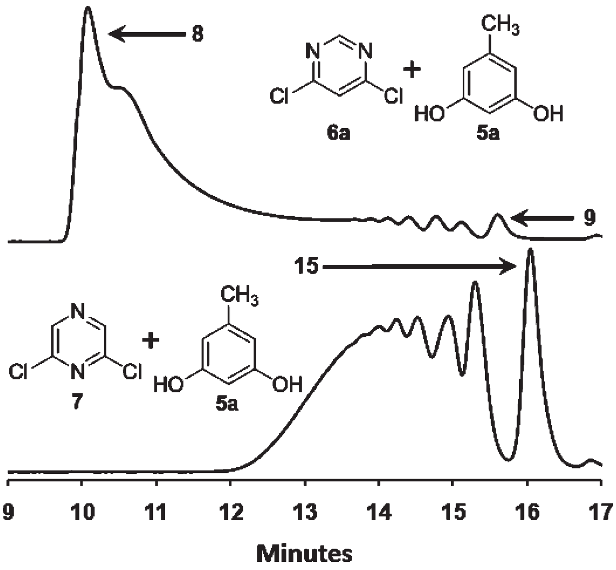

Figure 2. Mesopore GPC traces of the reactions of **5a** with **6a** (top) and **7** (bottom) analyzed after 8 min reaction times. Oxacalix[4]arene **9**, poly(*m*PO) **8**, and oxacalix[4]arene **15** are labeled.

Table 1. Scope of Synthesis and Yields of Various Poly(*m*POs) from Substituted *m*-Diphenols (5) and Dichloropyrimidines (6)[a]

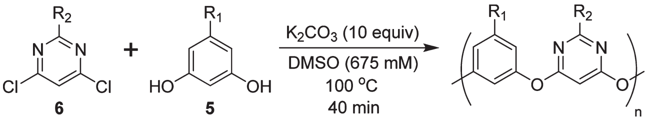

m-diphenol	pyrimidine	poly(*m*PO)	R_1	R_2	isolated yield (%)
5a	**6a**	**8**	CH_3	H	93
5b	**6a**	**10**	*n*-pentyl	H	87
5c	**6a**	**11**[b]	CO_2CH_3	H	92
5d	**6a**	**12**[c]	OCH_3	H	91
5b	**6b**	**13**	*n*-pentyl	SCH_3	87
5a	**6c**	**14**	CH_3	Ph	93

[a] Reaction conditions unless otherwise noted (10 equiv of K_2CO_3, DMSO, 40 min, 100 °C).[16] [b] Reaction was run for 3 h. [c] Reaction was run for 10 min at 80 °C.

(R_1 = OMe, **12**, 91%) substituent without significant decrease in yield. Incorporation of a diphenol substituted with a hydrocarbon chain such as in olivetol (**5b**) is useful for providing additional solubility to the polymer backbone. The observed rates of polymerization and equilibration correlated with the nucleophilicity of the *m*-diphenol monomer, and therefore time and temperature were altered accordingly to optimize kinetic poly(*m*POs) formation. The reaction time was lengthened (3 h) for the electron-poor *m*-diphenol **5c**, while both a lower reaction temperature (80 °C) and shorter reaction time (10 min) was optimal for the electron-rich *m*-diphenol **5d**. Furthermore, substitution is also tolerated at the 2-position of the pyrimidine electrophile (R_2 = SMe, **6b**, 87% or Ph, **6c**, 93%) using the standard reaction conditions, forming poly(*m*POs) **13** and **14**, respectively. Thus, a variety of pyrimidine-containing poly(*m*POs) are accessible under AA–BB type S_NAr conditions.

Effect of Electrophile Substitution. When 2,6-dichloropyrazine (**7**) is reacted with **5a** under the optimized conditions for the formation of **8**, none of the corresponding poly(*m*PO) is observed. GPC and ^1H NMR (Figure S4) analysis of the reaction mixture analyzed at 8 min, 30 min, and 20 h reaction times indicates that a mixture of cyclic and linear oligomers is formed, with oxacalix[4]arene **15** predominating both kinetically and thermodynamically. Figure 2 contains the GPC traces at 8 min reaction times for the condensation of **5a** with either **6a** (top) or **7** (bottom).[18] It is evident that, even at short reaction times, pyrimidine **6a** favors the formation of polymer while pyrazine **7** favors the formation of cyclic and linear oligomers.

Chart 1. Trimers 16–19 Synthesized from Orcinol 5a and Electrophiles 6a or 7

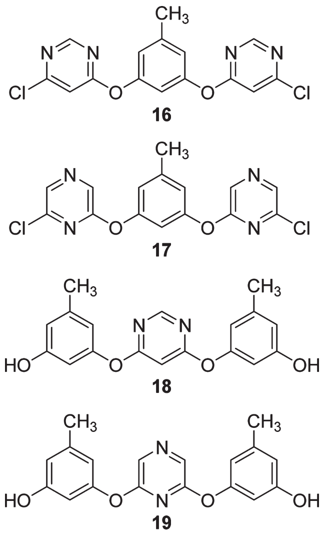

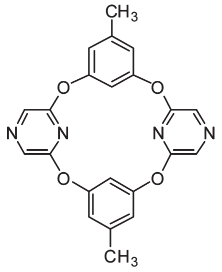

15

Linear trimers **16–19** (Chart 1) were synthesized to probe the differential reaction outcomes using electrophiles **7** and **6a**. The two electrophilic oligomers were terminated in chloropyrimidine (**16**) or chloropyrazine (**17**) with orcinol (**5a**) as the central unit. The two nucleophilic oligomers contained either pyrimidine (**18**) or pyrazine (**19**) as the central unit. We expected that combining electrophilic and nucleophilic trimers would remove a kinetic pathway for oxacalix[4]arene formation, biasing the production of either poly(*m*POs) or larger cyclic oligomers. Trimers **16** and **18** or **17** and **19** were combined under the optimized S_NAr polymerization conditions and analyzed by ^1H NMR (Figure S5 for **16** + **18** and Figure S6 for **17** + **19**) and GPC (Figure S7). Each reaction produced similar product mixtures as the analogous reactions using monomeric species.[19] The results from the reaction between **16** and **18** were consistent with a step-growth polymerization to form poly(*m*PO) **8**. However, in the pyrazine-containing systems, where oxacalix[4]arene **15** is predominantly formed, a kinetic cyclization pathway must be available even when starting with preformed trimers **17** and **19**. This pathway is most likely due to facile backbiting of the nucleophilic end of the requisite linear oligomeric chain on an internal pyrazine ring. While similar reactivities have been well documented in S_NAr-based polycondensation reactions with structurally related poly(aryl ethers),[20]

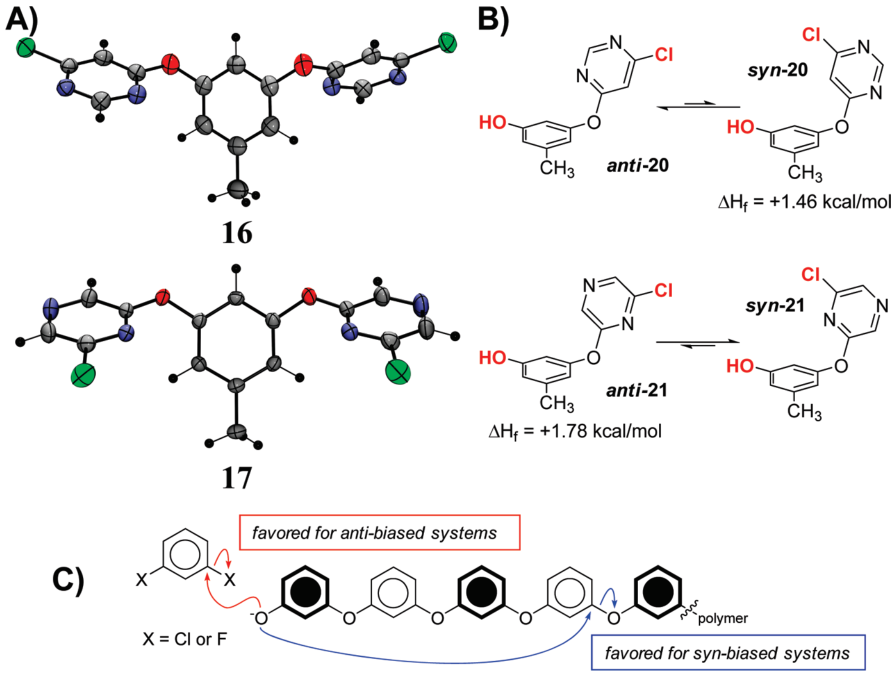

Figure 3. (A) X-ray crystal structure of trimers **16** and **17**. (B) Conformational preferences of dimers **20** and **21** from DFT calculations. (C) Mechanistic hypothesis for diverging kinetic S_NAr pathways for the reaction of nucleophilic *m*-diphenols (dark rings, **1**) and electrophilic aromatic *m*-dihalides (light rings, **2**).

backbiting ring closure has not previously been documented as an operative mechanistic pathway in oxacalixarene synthesis. Such a reaction pathway has the potential to significantly impact the reaction outcomes of fragment-coupling macrocyclization strategies that target large oxacalix[*n*]arenes as well as *m*PO polymerizations.

Modeling and Theory. It remained unresolved why the seemingly similar electrophiles 2,6-dichloropyrazine (**7**) and 4,6-dichloropyrimidine (**6a**) would exhibit such markedly different reaction paths under high concentration kinetic S_NAr conditions. A comparison of the X-ray crystal structures of trimers **16** and **17** provided initial insight that conformational differences of the linear oligomeric chains may be the source of the divergent reactivity (Figure 3A). While significant effort has been expended to determine oxacalix[4]arene conformation,[9,10] little has been disclosed with regard to ordering effects that control the conformations of the linear aryl ether precursors. In the solid state, trimer **16** adopts a conformation that orients the ring nitrogen over the adjacent aromatic ring while also maintaining conjugation between the bridging oxygen atoms and the pyrimidine rings (Figure 3A, $N_2-C_3-O_1-C_5$ dihedral angle of 15.38°). This preference causes an extended conformational bias for the trimer and orients the reactive chlorine atoms far apart in space. Strong conjugation between the bridging oxygen atoms and the pyrimidine rings is evident from analysis of the shortened C−O bond lengths (1.36 Å). Trimer **17** also adopts a solid-state conformation that places the ring nitrogen over the adjacent aromatic ring ($N_1-C_1-O_1-C_5$ and $N_3-C_{12}-O_2-C_9$ dihedral angles of −33.11° and 31.41°, respectively). However, for **17** this preference positions the chlorine atoms in close proximity, in a conformation that resembles the published solid-state structure of the corresponding oxacalix[4]arene (Figure S8).[9b]

Molecular mechanics (MMFF94x) and DFT (B3LYP/6-311+G**) calculations were conducted on dimeric species **20** and **21** and are in agreement with the observed solid-state conformational preferences for **16** and **17** (Figure 3B). Both dimers were calculated to energetically prefer orienting the ring nitrogen atoms, rather than a carbon atom bearing a hydrogen, over the adjacent aromatic ring (by 1.46 kcal/mol for **16** and 1.78 kcal/mol for **17**) while maintaining conjugation between the bridging oxygen atom and the electrophile-derived ring. The higher steric bulk of the C−H bond versus the nitrogen lone pair appears to be dominating factor in this conformational preference.[21] For pyrimidine-containing dimer **20**, the halogen on the electrophilic end is oriented away from the reactive phenol on the nucleophilic end (herein referred to as an *anti*-conformation). Conversely, pyrazine-containing dimer **21** is lowest energy when the halogen on the electrophilic end is oriented in close proximity to the reactive phenol on the nucleophilic end (herein referred to as a *syn*-conformation). Repetition of a *syn*-conformation would give rise to a polymer with a highly coiled local conformation, and the above experimental evidence suggests that backbiting cyclization to form the corresponding oxacalix[4]arene and other cyclic oligomers is competitive with chain growth. In contrast, polymer chains that contain electrophiles with an *anti*-conformational bias will adopt an extended local structure, minimizing backbiting at high electrophile concentrations and favoring chain growth to form poly(*m*POs).

More Evidence of Steric Control. Extension of our hypothesis, that kinetic product selectivity correlates with linear oligomer conformational preference, leads to the prediction that electrophiles substituted with sterically bulky groups at the 4- and 6-positions,[22] or bearing a ring nitrogen at the 2-position, will bias coiled linear oligomers (*syn*-conformational bias) and kinetically favor backbiting-induced oxacalixarene formation. Analogously, electrophiles bearing sterically bulky groups at the 2-position, or bearing ring nitrogens at the 4- and 6-positions, will bias extended linear oligomers (*anti*-conformational bias) and kinetically favor poly(*m*PO) formation. It is also consistent that, while 4,6-disubstituted electrophiles are common in oxacalix[4]arene synthesis,[9,10] there are no literature precedents of

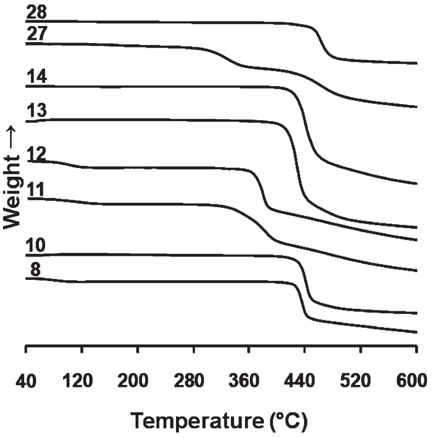

Figure 4. TGA of poly(*m*POs) **8**, **10**−**14**, **27**, and **28**.

Scheme 3. Syntheses of Poly(*m*POs) 27 and 28

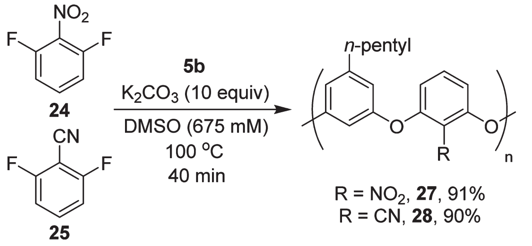

oxacalix[4]arene formation by $\mathrm{S_NAr}$ using 2-substituted electrophiles. However, the literature does contain one example of an oxacalix[6]arene[10h] formed in modest yield as well as the one previously reported poly(*m*PO) (**22**[7] and **23**[8]), synthesized from 2-subsituted electrophiles.

As a test to our hypothesis of electrophile-dependent polymerization, and to further expand the scope of accessible poly(*m*POs), the 2-substituted electrophiles 2-nitro-1,3-difluorobenzene (**24**) and 2,6-difluorobenzonitrile (**25**), and one previously reported[9b] 4,6-substituted electrophile, 2,3,5,6-tetrachloropyridine (**26**), were reacted with olivetol (**5b**), and the product distributions were analyzed. As expected, polymer formation was efficient using 2-substituted electrophiles **24** or **25**, and poly(*m*POs) **27** and **28** were isolated in 91% and 90% yield, respectively (Scheme 3). Also consistent with our prediction, 2,3,5,6-tetrachloropyridine (**26**) kinetically and thermodynamically formed the corresponding oxacalix[4]arene (and other oligomeric species) and did not form polymer as analyzed by ^{1}H NMR (Figure S9) and GPC (Figure S10).[16] Thus, in accordance with our electrophile-dependent model, base-induced AA−BB type $\mathrm{S_NAr}$-based polycondensation reactions can be used to produce a wide variety of poly(*m*POs).

Thermal Degradation and Stability. As previously stated, PPOs have traditionally been synthesized as thermally stable materials.[1−3] The thermal stabilities of poly(*m*POs) **8**, **10**−**14**, **27**, and **28** were analyzed by TGA (Figure 4) and DSC (Figure S11) under nitrogen up to 600 and 400 °C, respectively. These temperature ranges allow for comparisons to the previously published poly(*m*POs) **22**[7] and **23**[8] (Table 2) as well as the industrially produced PPO, poly(2,6-dimethyl-1,4-phenylene ether), which has a T_g of 205 °C and a T_m of 267 °C with a critical temperature of 428 °C,[2] and to other non-halogen-containing PPOs that show good stability at 400 °C but significant weight loss above 400 °C.[3a]

Figure 4 shows that all poly(*m*POs) synthesized exhibit thermal stabilities above 300 °C by TGA. The thermal stabilities appear to have a correlation to molecular weight[23] (Figure S12) regardless of the substitution on the polymer backbone. The higher molecular weight orcinol-derived poly(*m*POs) **8** and **14** showed no phase transitions by DSC and less than 5% weight loss at 420 °C by TGA. Lower molecular weight poly(*m*POs) **11** and **12**, bearing carbomethoxy and methoxy functionality, respectively, also showed no phase transitions by DSC but displayed reduced thermal stability by TGA with decomposition occurring at 321 °C for **11** and 350 °C for **13**. The olivetol-derived poly(*m*POs) were the only polymers to exhibit phase transitions by DSC, most likely because the *n*-pentyl hydrocarbon side chains facilitate polymer reorganization. Poly(*m*POs) **10**, **13**, **27**, and **28** were found to have T_m values of 76, 46, 91, and 206 °C, respectively. The 2-substituted poly(*m*POs) exhibit additional features (Table 2) that the pyrimidine-containing polymers do not. Poly(*m*PO) **27** has a T_g at 65 °C, and poly(*m*PO) **28** has a T_g at 79 °C and a T_c at 133 °C. The T_g and T_m values observed for poly(*m*POs) **27** and **28** were expected to be lower than that for **22** and **23** because of the *n*-pentyl side chain. Thus, by tuning the appended side chains and possibly the molecular weight, a wide range of poly(*m*POs) may be synthesized to exhibit desired thermal and other physical properties.

Table 2. Properties of 2-Substituted Poly(*m*POs) 22, 23, 27, and 28

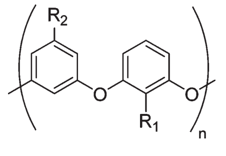

poly(*m*PO)	R_1	R_2	T_g (°C)	T_m (°C)	T_d (°C)	reference
22	CN	H	148	340	480[a]	7
23	CN	H	147	335	not reported	8
27	NO_2	*n*-pentyl	65	91	305[b]	
28	CN	*n*-pentyl	79	206	430[b]	

[a] 5% weight loss temperature in air. [b] 5% weight loss temperature under nitrogen.

The chemical stability of poly(*m*PO) **8** was also investigated in alkaline solutions. Under conditions similar to those used for the polycondensation, poly(*m*PO) **8** was placed in a flask with DMSO and 4 equiv (relative to the repeat units) of K_2CO_3. This heterogeneous solution[14] was heated to 100 °C for 24 h, at which point ^{1}H NMR analysis (Figure S13) revealed complete conversion to oxacalix[4]arene **9**. However, when poly(*m*PO) **8** is combined with 10 equiv of NaOH in water and heated at 100 °C for 7 days, quantitative recovery of poly(*m*PO) **8** was observed. These results indicate that poly(*m*PO) **8** can depolymerize in polar aprotic solvents to the thermodynamically more stable oxacalix[4]arene **9** but display robust aqueous stability even in a highly alkaline solution.

Conclusions

We have shown that base-induced $\mathrm{S_NAr}$ polycondensation reactions can be used to generate a range of poly(*m*POs), including those containing heteroaromatic rings in the polymer backbone. Mechanistic investigations have also revealed that successful polymerization requires the use of electrophilic monomers that enforce an extended local conformational bias (*anti*-conformation) to minimize cyclooligomer production through competing backbiting cyclization. Local conformational preferences of the growing oligomeric chain correlate with the substitution pattern of the electrophilic monomer, and a model has been described that allows facile prediction of reaction outcomes for a given electrophilic substrate. As reported for many other

AA−BB polycondensation processes,[20,24] we found that in certain cases (i.e., *syn*-biased systems) the observed product ratios do not follow classical theory[25] for the relationship between concentration and the resulting macrocycle to polymer ratio. Depending on the substitution pattern on the electrophilic monomer, macrocycle formation is kinetically driven to favor macrocycles regardless of concentration.

The synthesized poly(*m*POs) display a wide range of thermal behavior, including in several cases high thermal stabilities, and robust resistance to aqueous basic conditions. Future work will focus on extending the scope of materials available through our method, controlling and optimizing the molecular weights of desirable polymers, as well as optimizing the thermal and oxidative stabilities of these materials.

Acknowledgment. We are grateful to Dr. Susan Odom and Prof. Jeffery Moore for analytical GPC analysis in THF, Nagamani Chikkannagari and Prof. Sankaran Thayumanavan for TGA, and Prof. Elizabeth Stemmler for MALDI mass spectral analysis of compounds **16** and **17**. This work is supported by the National Science Foundation (CHE-0640729, CHE-0552292, MRI-0116416), Research Corporation (CC6665), the Petroleum Research Fund (45440-B1), and Colby College.

Supporting Information Available: Computation data tables for compounds **20** and **21**, crystallographic data for compounds **16** and **17**, detailed experimental procedures and characterization for all discussed compounds, and additional ^{1}H NMR, GPC, TGA, and DSC data of poly(*m*POs) and oxacalix-[4]arenes. This material is available free of charge via the Internet at http://pubs.acs.org.

References and Notes

(1) (a) Price, C. C. In *The Chemistry of the Ether Linkage*; Patai, S., Ed.; Interscience: New York, 1967; pp 499−523. (b) Maiti, S.; Mandal, B. K. *Prog. Polym. Sci.* **1986**, *12*, 111–153. (c) Jayakannan, M.; Ramakrishnan, S. *Macromol. Rapid Commun.* **2001**, *22*, 1463–1473. (d) Higashimura, H.; Fujisawa, K.; Moro-oka, Y.; Kubota, M.; Shiga, A.; Terahara, A.; Uyama, H.; Kobayashi, S. *J. Am. Chem. Soc.* **1998**, *120*, 8529–8530. (e) Jurek, M. J.; McGrath, J. E. *Polym. Prepr.* (*Am. Chem. Soc., Div. Polym. Chem.*) **1987**, *28*, 180–181.

(2) Aycock, D.; Abolins, V.; White, D. M. *Encyclopedia of Polymer Science and Engineering*, 2nd ed.; John Wiley & Sons: New York, 1986; Vol. *13*, pp 1−30.

(3) (a) Labadie, J. W.; Hedrick, J. L.; Ueda, M. In *Step-Growth Polymers for High-Performance Materials, New Synthetic Methods*; Hedrick, J. L., Labadie, J. W., Eds.; ACS Symposium Series 624; American Chemical Society: Washington, DC, 1996; pp 210−225. (b) Cotter, R. J. In *Engineering Plastics, A Handbook of Polyarylethers*; Gordon and Breach: Basel, Switzerland, 1995; Chapter 1.

(4) AA−BB type polymerization: (a) Kim, Y. J.; Chung, I. S.; Kim, S. Y. *Macromolecules* **2003**, *36*, 3809–3811. AB-type polymerization: (b) Suzuki, Y.; Hiraoka, S.; Yokoyama, A.; Yokozawa, T. *J. Polym. Sci., Part A: Plym. Chem.* **2004**, *42*, 1198–1207. (c) Yokozawa, T.; Suzuki, Y.; Hiraoka, S. *J. Am. Chem. Soc.* **2001**, *123*, 9902–9903.

(5) (a) Lim, P. K.; Huss, A.; Eckert, C. A. *J. Phys. Chem.* **1982**, *86*, 4233–4237. (b) Steenken, S.; Neta, P. *J. Phys. Chem.* **1982**, *86*, 3661–3667.

(6) (a) Cox, J. M.; Wright, B. A.; Wright, W. W. *J. Appl. Polym. Sci.* **1965**, *9*, 513–522. (b) Beeson, J. H.; Pecsar, R. E. *Anal. Chem.* **1969**, *41*, 1678–1682.

(7) (a) Matsuo, S.; Murakami, T. European Patent 192,177, U.S. Patent 4,703,104, **1986**. (b) Matsuo, S.; Murakami, T.; Takasawa, R. *J. Polym. Sci., Part A: Polym. Chem.* **1993**, *31*, 3439–3446.

(8) Kricheldorf, H. R.; Meier, J.; Schwarz, G. *Makromol. Chem., Rapid Commun.* **1987**, *8*, 529–534.

(9) (a) Katz, J. L.; Feldman, M. B.; Conry, R. R. *Org. Lett.* **2005**, *7*, 91–94. (b) Katz, J. L.; Geller, B. J.; Conry, R. R. *Org. Lett.* **2006**, *8*, 2755–2758. (c) Katz, J. L.; Geller, B. J.; Foster, P. D. *Chem. Commun.* **2007**, 1026–1028.

(10) (a) Sommer, N.; Staab, H. A. *Tetrahedron Lett.* **1966**, *25*, 2837–2841. (b) Lehmann, F. P. A. *Tetrahedron* **1974**, *30*, 727–733. (c) Gilbert, E. E. *J. Heterocycl. Chem.* **1974**, *11*, 899–904. (d) Bottino, F.; Foti, S.; Papalardo, S. *Tetrahedron* **1976**, *32*, 2567–2570. (e) Chambers, R. D.; Hoskin, P. R.; Kenwright, A. R.; Khalil, A.; Richmond, P.; Sandford, G.; Yufit, D. S.; Howard, J. A. K. *Org. Biomol. Chem.* **2003**, *1*, 2137–2147. (f) Wang, M.-X.; Yang, H.-B. *J. Am. Chem. Soc.* **2004**, *126*, 15412–15422. (g) Hao, E.; Fronczek, F. R.; Vicente, M. G. H. *J. Org. Chem.* **2006**, *71*, 1233–1236. (h) Yang, F.; Yan, L.; Ma, K.; Yang, L.; Li, J.; Chen, L.; You, J. *Eur. J. Org. Chem.* **2006**, 1109–1112. (i) Konishi, H.; Tanaka, K.; Teshima, Y.; Mita, T.; Morikawa, O.; Kobayashi, K. *Tetrahedron Lett.* **2006**, *47*, 4041–4044. (j) Maes, W.; Van Rossom, W.; Van Hecke, K.; Van Meervelt, L.; Dehaen, W. *Org. Lett.* **2006**, *8*, 4161–4164. (k) Konishi, H.; Mita, T.; Morikawa, O.; Kobayashi, K. *Tetrahedron Lett.* **2007**, *48*, 3029–3032. (l) Jiao, L.; Hao, E.; Fronczek, F. R.; Smith, K. M.; Vicente, M. G. H. *Tetrahedron* **2007**, *63*, 4011–4017. (m) Wang, M.-X. *Chem. Commun.* **2008**, 4541–4551. (n) Maes, W.; Dehaen, W. *Chem. Soc. Rev.* **2008**, *37*, 2393–2402. (o) Ma, M.-L.; Wang, H.-X.; Li, X.-Y.; Liu, L.-Q.; Jin, H.-S.; Wen, K. *Tetrahedron* **2009**, *65*, 300–304. (p) Van Rossom, W.; Ovaere, M.; Van Meervelt, L.; Dehaen, W.; Maes, W. *Org. Lett.* **2009**, *11*, 1681–1684.

(11) The only notable exception being poly(arylene ether nitrile), refs 7 and 8.

(12) We include 6-membered heteroaromatic rings in our definition of *m*PO.

(13) Molecular weights for the polymers in this paper are reported in the experimental section of the Supporting Information but are not otherwise discussed because our synthetic optimization focused on yield and not molecular weight. Additionally, the monomers were used as received in varying degrees of purity. See Supporting Information for reported purities.

(14) Poly(*m*PO) **8** precipitates out of solution during the polymerization, and purified **8** is only slightly soluble in DMSO.

(15) The use of DMF as the solvent under optimized conditions afforded *m*PO **8** in 88% isolated yield with a M_n of 26 100 and PDI of 2.51, and the reaction mixture contains 8% oxacalix[4]arene **9** prior to purification as analyzed by ^{1}H NMR.

(16) See the Supporting Information for full details

(17) Throughout the paper and Supporting Information we show ^{1}H NMRs and indicate the peak to which each spectrum is referenced. This is necessary because, as shown in Figure S2, significant peak shifting is observed depending on the environment of the polymer.

(18) The Mesopore (Varian, Inc.) columns used for Figure 2 and in the Supporting Information have a molecular weight cutoff of 25 kDa. Poly(*m*PO) **8** is partially above this molecular weight range, and the GPC chromatogram shown in Figure 2 should only be used as a qualitative comparison of the formed oligomers. Analytical GPC was performed to determine the molecular weights of the poly-(*m*POs) using Vistotek Viscogel columns with a higher molecular weight range (see the Supporting Information for more details). All analytical GPC traces of poly(*m*POs) are monomodal (i.e., the bimodal appearance of some high molecular weight peaks from the Mesopore GPC arises from the molecular weight cutoff of the column).

(19) It is worth noting that, relative to the monomer reaction (**7** + **5a**), the condensation of **17** + **19** does show an increase in the amount of oxacalix[6]arene formed, but the ^{1}H NMR and GPC are otherwise very similar.

(20) (a) Kricheldorf, H. R.; Rabenstein, M.; Maskos, M.; Schmidt, M. *Macromolecules* **2001**, *34*, 713–722. (b) Kricheldorf, H. R.; Böhme, S.; Schwarz, G. *Macromolecules* **2001**, *34*, 8879–8885. (c) Kricheldorf, H. R.; Böhme, S.; Schwarz, G.; Krüger, R.-P.; Schulz, G. *Macromolecules* **2001**, *34*, 8886–8893. (d) Kricheldorf, H. R.; Böhme, S.; Schwarz, G.; Schultz, C.-L. *Macromol. Rapid Commun.* **2002**, *23*, 803–808.

(21) The angle distortion, torsional distortion, and van der Waals steric energies were consistently the dominant factors in comparing calculated ΔH_f values for the *syn*- vs *anti*-conformations of **20** and **21** when energy minimized at the MMFF94x level (see the computation data tables for dimers **20** and **21** in the Supporting Information).

(22) To simplify the comparison, positional numbering in this section assumes that the carbon atoms bearing halogen atoms in all electrophiles will be numbered positions 1 and 3. Thus, substitution at the 2-position refers to the position between the reactive halogens on the electrophile monomers, irrespective of IUPAC priority weighting.

(23) Molecular weights for all polymers are reported in the Supporting Information except poly(*m*PO) **28**, which was not soluble in THF. Previously reported polymers **22** and **23** do not have reported molecular weights.

(24) Yokozawa, T.; Ajioka, N.; Yokoyama, A. *Adv. Polym. Sci.* **2008**, *217*, 1–77.

(25) Flory, P. J. *Principles of Polymer Chemistry*; Cornell University Press: Ithaca, NY, 1953.